Temperature dependence of the electron paramagnetic resonance spectra of Mn^{2+} impurity ions in $PbWO_4$ single crystals

2005 J. Phys.: Condens. Matter 17 719

(http://iopscience.iop.org/0953-8984/17/4/014)

INSTITUTE OF PHYSICS PUBLISHING JOURNAL OF PHYSICS: CONDENSED MATTER

J. Phys.: Condens. Matter **17** (2005) 719–728 doi:10.1088/0953-8984/17/4/014

Temperature dependence of the electron paramagnetic resonance spectra of Mn^{2+} impurity ions in $PbWO_4$ single crystals

M Stefan[1,4], S V Nistor[1], E Goovaerts[2], M Nikl[3] and P Bohacek[3]

[1] National Institute for Materials Physics, POB MG-7 Magurele-Bucharest, RO-077125, Romania
[2] Department of Physics, University of Antwerpen, Campus Drie Eiken, Universiteitsplein 1, BE-2610 Antwerpen, Belgium
[3] Institute of Physics AS CR, Cukrovarnicka 10, 16200 Prague 6, Czech Republic

E-mail: mstefan@infim.ro

Received 29 November 2004
Published 14 January 2005
Online at stacks.iop.org/JPhysCM/17/719

Abstract

The temperature variation of the fine and hyperfine parameters of Mn^{2+} in single crystals of $PbWO_4$ in the low temperature range reveals the presence of a resonant mode of frequency $\omega = 8.8 \times 10^{12}$ rad s^{-1}. Moreover, above 60 K, where the temperature induced broadening becomes dominant, a T^{-2} variation of the relaxation time was inferred from the analysis of the temperature dependence of the Mn^{2+} linewidth. This variation is attributed to a Raman relaxation process due to the coupling with the same local resonant mode.

1. Introduction

Lead tungstate—$PbWO_4$ (PWO)—is at present one of the most studied materials in scintillator oriented research, due to its approved applications in the detectors of high-energy physics accelerators (projects CMS and ALICE at the Large Hadron Collider in CERN). The achieved results in understanding the microscopic nature of the energy transfer and storage processes in PWO were recently reviewed [1]. A crucial issue in the optimization of PWO for the above applications was achieved by the selected trivalent ion doping at the Pb^{2+} site, which efficiently compensated/suppressed the intrinsic trapping states in the forbidden gap of PWO [2–4]. However, other research to obtain PWO of higher scintillation efficiency is intensively going on and is based on the multiply doped [5], stressed or nonstoichiometric [6] crystals. Thus, one of the main aspects of the research on this compound concerns the point defect properties (localization, structure, quantum states) and their influence on the energy balance and scintillating properties of the single-crystalline PWO. Alternatively, paramagnetic point defects in the form of transition metal ions in small (a few ppm) concentrations can be

[4] Author to whom any correspondence should be addressed.

used as atomic probes in investigating both static and dynamic properties of the host lattice local crystal field.

The electron paramagnetic resonance (EPR) spectra of the Mn^{2+} ions in PWO single crystals have only recently been reported [7]. It was found that Mn^{2+} ions enter the crystal lattice substitutionally at Pb^{2+} sites. The presence of random lattice strains was also inferred from the angular variation of the observed EPR linewidth, which could affect the optical properties of the crystals as well. The present work expands these investigations and focuses on the influence of the temperature on the Mn^{2+} EPR spectra and the further information that can be gained from it about the dynamic crystal lattice properties, in particular the spin–lattice interaction with the dispersed Mn^{2+} impurity ions.

2. Experimental details

The symmetry of the PWO crystal, as a member of the scheelite family, is described by the tetragonal space group $I4_1/a(C_{4h}^6)$ and the point group $4m$, with four molecules per unit cell. The lattice constants are $a = b = 0.5455$ nm and $c = 1.2027$ nm. The structure consists of slightly distorted WO_4^{2-} tetrahedra, with Pb^{2+} ions interspersed among them [8]. Each Pb^{2+} ion is surrounded by eight O^{2+} ions. The point symmetry at both Pb^{2+} and W^{4+} sites is S_4.

The crystals used in this work have been grown by the Czochralski technique. As in the early study [7], we have used undoped, as well as Sn (300 ppm) and Bi (600 ppm) doped, single crystals, all grown along the c crystalline direction. Oriented EPR samples of about $2.4 \times 2.4 \times 10$ mm^3 size were cut from these crystals, with the long/rotation axis along one of the a or c crystal axes.

The EPR measurements were carried out with a Bruker ESP 300E X-band spectrometer, equipped with a gas-flow cryogenic system (ESR910 from Oxford Instruments), allowing operation in the 1.5–290 K temperature range. Because of the large difference (of up to 10 K) between the temperature indicated by the temperature controller of the ESR910 system and the temperature at the sample position measured directly with a separate sensor, a difference which we found to depend also on the gas flow and heater regime, we built a sample holder equipped with a chromel–AuFe (0.07%) thermocouple [9] installed above, in the vicinity of the sample. By averaging the two temperature readings (from the controller and sample holder), an estimated accuracy of ± 1 K in the temperature determination at the sample location could be obtained. The numerical analysis of the observed EPR spectra was performed with the EPRNMR (version 6.5) computer program [10].

3. EPR measurements

The experiments performed on all three types of PWO single crystals revealed the presence of EPR spectra composed of 30 narrow lines, visible up to room temperature, attributed to Mn^{2+} ions, present in the crystal lattice as an unintentional impurity. The comparable intensity of the EPR spectra in the undoped and both Sn and Bi doped PWO crystals strongly suggests that the small quantities of manganese originate in the PbO and/or WO_3 starting materials. Although the exact concentration of Mn^{2+} in the resulting single crystals has not been determined, one estimates a concentration of less than 1 ppm. Other EPR transitions, which could be observed in all examined samples, have been attributed to comparable, or even smaller, concentrations of Gd^{3+} [11], Ce^{3+} and Nd^{3+} [12] and other, as yet unidentified, paramagnetic impurity ions. Some of these transitions have been used for the accurate orientation of the measured samples in the magnetic field.

The EPR spectra of Mn^{2+} were found to be very similar in the three differently doped crystals, and thus the originating crystal will not be further mentioned. The EPR lines attributed

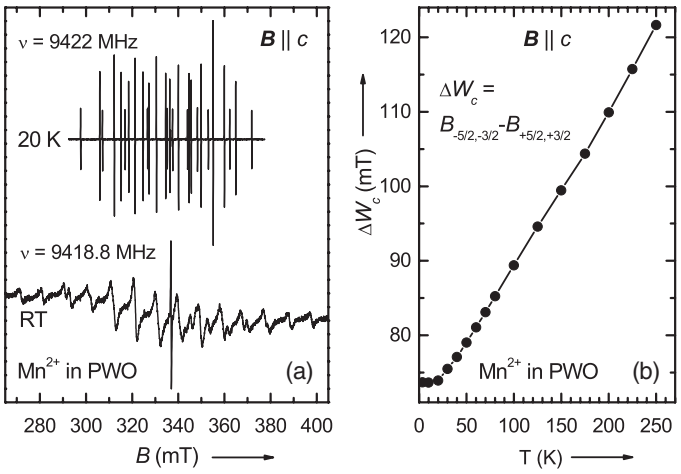

Figure 1. (a) The EPR spectra of the Mn^{2+} ions in the PWO crystals recorded in the X-band for the $\boldsymbol{B} \parallel c$ orientation, at $T = 20$ K and at room temperature (RT), respectively. (b) The temperature variation of the magnetic field range covered by the Mn^{2+} spectrum, $\Delta W_c = B_{-5/2,-3/2} - B_{+5/2,+3/2}$, for the $\boldsymbol{B} \parallel c$ orientation.

to the Mn^{2+} ions exhibit a strong temperature induced variation in the field positions, the spectrum tending to expand monotonically with increasing temperature, which is accompanied by a simultaneous line broadening effect (see figures 1(a) and (b)). This strong temperature variation of the spectrum magnetic field range did allow us to use the Mn^{2+} spectrum as a secondary temperature etalon (thermometer) in those experiments where the thermocouple-equipped holder could not be used. This was accomplished by using the maximum magnetic field range of the Mn^{2+} spectrum along the c and a directions $\Delta W_c = |B_{-5/2,-3/2} - B_{+5/2,+3/2}|$ versus T dependence (see figure 1(b)), measured with the thermocouple equipped holder, as the calibration curve for temperature determinations in the other experiments. This way we achieved an accuracy in the temperature determination comparable with that obtained by using the specially designed holder.

The most accurate set of EPR parameters of Mn^{2+} has been determined at 20 K [7], by fitting the angular dependence of the EPR spectra in the (ac), (ab) and (110) planes to the following spin Hamiltonian (SH), with usual notations [13]:

$$(1/g_0\mu_B)\mathcal{H} = (1/g_0)\boldsymbol{S}\cdot\boldsymbol{g}\cdot\boldsymbol{B} + B_2^0\cdot\boldsymbol{O}_2^0 + B_4^0\cdot\boldsymbol{O}_4^0 + B_4^4\cdot\boldsymbol{O}_4^4 + B_4^{-4}\cdot\boldsymbol{O}_4^{-4} + \boldsymbol{S}\cdot\boldsymbol{A}\cdot\boldsymbol{I} - (g_n\mu_N/g_0\mu_B)\boldsymbol{B}\cdot\boldsymbol{I} + \boldsymbol{I}\cdot\boldsymbol{Q}\cdot\boldsymbol{I}. \quad (1)$$

Here $S = I = 5/2$ and the reference frame corresponds to the crystal axes a, b and c. It has also been found [7] that the spectra exhibit tetragonal symmetry, with the magnetic tetragonal axis z parallel to the c crystal direction, and the magnetic x axis lying at about 7° from the a direction in the (ab) plane. By performing the SH parameters determination in the local magnetic xyz reference system, the B_4^{-4} parameter cancels and a simpler SH, in which the $B_4^{-4}\cdot\boldsymbol{O}_4^{-4}$ term is missing, is obtained. The resulting SH parameters, determined at $T = 20$ K, with such a simplified SH, are given in table 1. The same simplified SH has been further employed in the present temperature dependence study of the SH parameters. The signs of the B_n^m and of the hyperfine parameters A and Q have been taken by reference to the sign of the B_2^0 parameter, which was considered to be negative, in agreement with early results in other scheelite compounds such as $CaWO_4$ [14] and $SrWO_4$ [15]. The observed anisotropy of the g-factor, although small, is real and not merely a calculation artefact, as further demonstrated

Table 1. The spin Hamiltonian (SH) parameters of the Mn^{2+} ions in $PbWO_4$ at 20 K [7] and 80 K (this work) in comparison with similar data in the isostructural $CaWO_4$ crystals. The SH is expressed in the local magnetic coordinate system *xyz*, with $z \parallel c$ and x at 7° (PWO) and 9° ($CaWO_4$), respectively, from the a axis in the (ab) plane.

SH parameters	Mn^{2+} in $PbWO_4$ $T = 20$ K	Mn^{2+} in $PbWO_4$ $T = 80$ K	Mn^{2+} in $CaWO_4$ $T = 80$ K[a]
$g_\parallel$	2.0004 ± 0.0001	2.0008 ± 0.0001	2.00006 ± 0.00005
$g_\perp$	2.0002 ± 0.0001	2.0004 ± 0.0001	2.00079 ± 0.00006
B_2^0 (mT)	$-(1.042 \pm 0.005)$	$-(1.508 \pm 0.005)$	$-(4.912 \pm 0.002)$
B_4^0 (mT)	$-(0.0024 \pm 0.0005)$	$-(0.0024 \pm 0.0005)$	$-(0.0026 \pm 0.0002)$
B_4^4 (mT)	$-(0.0123 \pm 0.0003)$	$-(0.0141 \pm 0.0005)$	$-(0.0186 \pm 0.0002)$
$A_\parallel$ (mT)	$-(9.540 \pm 0.005)$	$-(9.510 \pm 0.005)$	$-(9.524 \pm 0.006)$
$A_\perp$ (mT)	$-(9.637 \pm 0.005)$	$-(9.602 \pm 0.005)$	$-(9.592 \pm 0.006)$
Q (mT)	$-(0.044 \pm 0.005)$	$-(0.044 \pm 0.005)$	$-(0.032 \pm 0.003)$

[a] Data reported in [16]. The conversion from b_4^m to B_4^m has been incorrectly done and presented in [7].

by the analysis of the temperature dependence of the EPR spectra. The similar local symmetry and valence state of the Mn^{2+} impurity ions and Pb^{2+} lattice cations lead to the conclusion that the Mn^{2+} ions entered the PWO crystal lattice substitutionally at Pb^{2+} sites, during the crystal growth process.

We have previously found out that the random lattice strains induce a significant broadening of the EPR lines of the Mn^{2+} in PWO which did not belong to the central sextet [7]. The low concentration of the Mn^{2+} ions thus proved to be an advantage, as in the absence of significant dipolar interaction the fine structure transitions $1/2 \leftrightarrow -1/2$ exhibited linewidths as narrow as 0.062 mT below $T = 10$ K. When the magnetic field was rotated away from the crystal axes, the $\pm 1/2 \leftrightarrow \pm 3/2$ and $\pm 3/2 \leftrightarrow \pm 5/2$ fine structure transition lines broadened very fast and at angles larger than 20° they could hardly be observed anymore. At higher temperatures the relaxation induced line-broadening leads to a further decrease of the visibility range for the non-central sextet transitions. Thus, above 100 K they could be observed only for orientations very close to the crystal axes.

The linewidths also limited the accuracy in the line positions and corresponding SH parameter determination. Up to 100 K the line positions could be determined with an accuracy of ± 0.03 mT. At higher temperatures the accuracy in the determination of the transition fields for the lines which did not belong to the central sextet decreased, due to both thermal broadening and superposition of lines. Consequently, the accuracy of the fit decreased, especially in the determination of the parameters with a smaller absolute value. The effects were larger along the a direction, for which, above 200 K, it was not possible to distinguish the $\pm 1/2 \leftrightarrow \pm 3/2$ and $\pm 3/2 \leftrightarrow \pm 5/2$ fine structure transition lines and thus to determine the fine and hyperfine perpendicular parameters.

For the current temperature variation study the measurements were carried out along the a and c main crystalline directions. Because the variable temperature system we have employed did not allow us to set the real temperature accurately, the sampled temperatures for the measurements along the two distinct directions generally did not coincide, as the measurements were performed on two differently oriented samples. Thus the analysis was performed in several steps: for a few common temperatures (up to 80 K) the fit was performed on data from both axes, simultaneously, and a common set of parameters was obtained. For the other sampled temperatures the axial and perpendicular parameters were determined by simulating and fitting the spectra along the c and a axes separately.

The simulation of the spectra along the c direction required a smaller number of 'parallel' parameters, namely $g_\parallel$, B_2^0, B_4^0 and $A_\parallel$, which were allowed to vary freely during the fitting

procedure. For simulating the spectra along the a direction, at a specific temperature, the 'parallel' parameters were calculated by interpolation from the values determined along the c direction and only the 'perpendicular' parameters ($g_\perp$, B_4^4 and $A_\perp$) were allowed to vary freely. The Q parameter was kept fixed at the value determined at 20 K. The resulting SH parameter values determined by this procedure were found to be in very good agreement with the parameter values determined by fitting the data on both axes simultaneously at coincident temperatures.

Table 1 also presents the SH parameters for the Mn^{2+} ions in the isostructural $CaWO_4$ crystals at 80 K [16], together with the corresponding set of parameters determined at the same temperature in PWO, using the above mentioned procedure. In the case of the of the Mn^{2+} centre in $CaWO_4$ the EPR spectrum was also described with the simplified SH, the local magnetic x direction being at about 9° from the a axis in the (ab) plane [14]. One can notice that the largest difference between the two sets of data at 80 K corresponding to the two host crystals appears in the B_2^0 parameter's value, pointing to a stronger axial component of the local crystal field on the Mn^{2+} in $CaWO_4$.

4. Results and discussions

The temperature dependence of the EPR parameters is expected to arise from both implicit and explicit effects. The implicit effects, namely the thermal expansion, could not be directly (quantitatively) accounted for because of the absence of corresponding data for the PWO lattice at temperatures below RT. However, previous analysis of the temperature variation of the Mn^{2+} fine and hyperfine parameters in various host lattices showed [17–21] that the explicit contributions, i.e. from the lattice vibrations, are dominant. Therefore, in the following analysis, the thermal expansion contribution to the zero-field splitting (ZFS) and hyperfine parameters is considered negligible and the coupling with the lattice vibrations is considered responsible for the observed variations.

4.1. The anisotropy of the g-factor

The g-factor values for both a- and c-axes exhibit a monotonic and close to linear decrease with the temperature (see figures 2(a) and (b)). The relative variation is very small but nonetheless present. The temperature dependence of the g-factors is supposed to result mainly from the lattice expansion [17], being due to the spin–orbit coupling, and therefore it is expected to be of the form T^n. Indeed, we could fit the experimental data with such a function:

$$g(T) = g_0 + g_1 T^n \tag{2}$$

where $n = 1.1$ for both $g_\parallel$ and $g_\perp$. The other parameters were found to be $g_0 = 2.0009 \pm 0.0001$ and $g_1 = (-10 \pm 7) \times 10^{-7}$ for $g_\parallel$, and $g_0 = 2.0005 \pm 0.0001$ and $g_1 = (-8 \pm 7) \times 10^{-7}$ for $g_\perp$, respectively.

4.2. The temperature dependence of the B_2^0 parameter

The fine structure parameter B_2^0 is the largest ZFS parameter and the most sensitive one to changes in the local axial crystalline field component. It exhibits the best-defined temperature variation. There is a strong increase of the absolute value of the B_2^0 parameter with increasing temperature (see figure 3). This is partly expected to result from the different values of the thermal expansion coefficients along the c and a directions [22], which would lead to an increased axiality. However, as previously mentioned, the temperature dependence of B_2^0 is

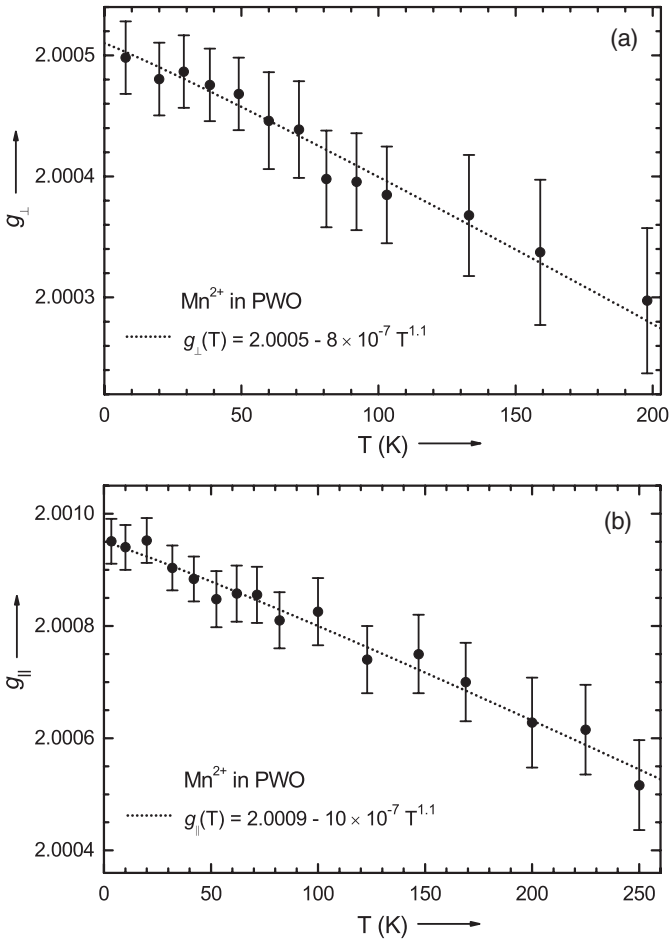

Figure 2. The temperature variation of the (a) $g_\perp$ and (b) $g_\parallel$ parameters for the Mn^{2+} ions in PWO. Solid circles: experimental data. Dotted line: simulated temperature dependence.

attributed mostly to the explicit effects of the lattice dynamics or/and to the possible presence of a resonant mode [19, 20]. In view of the large difference between the masses of the Mn^{2+} and Pb^{2+} ions, the second explanation appears to be the best suited.

By considering only the influence of a resonant mode, $|B_2^0|(T)$ can be fitted [20] with a function of the form

$$|B_2^0|(T) = \beta_0 + \beta_1 \coth(\hbar\omega/2k_{\mathrm{B}}T). \tag{3}$$

Here the first term is the parameter value at 0 K and the second term represents the coupling of the Mn^{2+} ion with a resonant mode of frequency ω.

The fitting parameters were found to be $\beta_0 = 0.70 \pm 0.02$ mT, $\beta_1 = 0.31 \pm 0.03$ mT and $\omega = (8.8 \pm 0.6) \times 10^{12}$ rad s^{-1}. The resulting fitting curve is represented with a dotted curve in figure 3. It shows that the local mode is strong enough to be practically responsible for the coupling of the spin of the manganese ions with the crystal lattice [23]. We have also tried to fit the experimental data by considering the influence of all lattice vibrations [17], but the result was less precise, especially at lower temperatures (below ∼30 K).

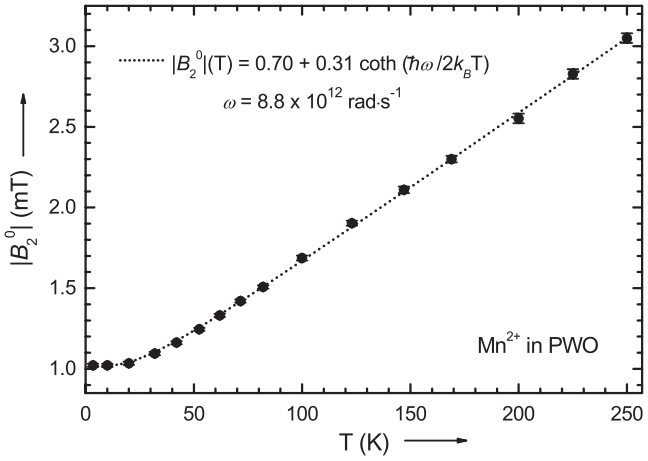

Figure 3. The temperature variation of the absolute value of the B_2^0 parameter for the Mn^{2+} ions in PWO. Solid circles: experimental data. Dotted curve: simulated temperature dependence.

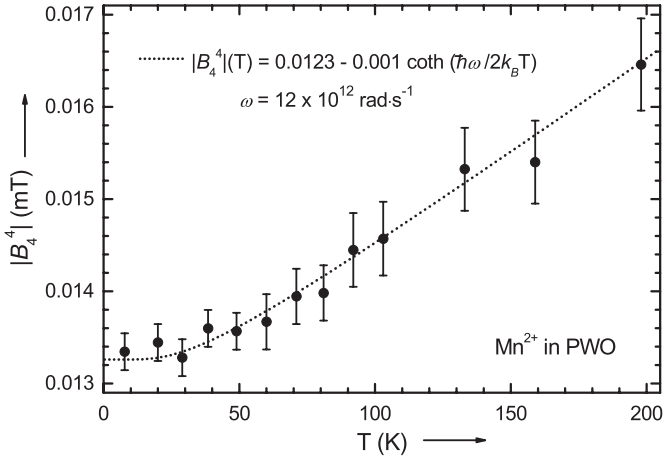

Figure 4. The temperature variation of the absolute values of the B_4^4 parameter for the Mn^{2+} ions in PWO. Solid circles: experimental data. Dotted curve: simulated temperature dependence.

4.3. The temperature dependence of the B_4^0 and B_4^4 parameters

The B_4^0 parameter was found to be practically constant in the investigated temperature range, with a value of $-(0.0024 \pm 0.0005)$ mT. On the other hand, the absolute value of the B_4^4 parameter exhibits a clear increase with the temperature, as one can see in figure 4. Although the errors in the determination of this parameter were quite large, its variation with temperature could be still determined. The presence of a local mode is expected to affect this parameter in the same way as it affects the B_2^0 parameter and, thus, the temperature dependence could be described by a relation similar to the expression (3). The fitting parameters were found to be $\beta_0 = 0.0123 \pm 0.0003$ mT, $\beta_1 = 0.0010 \pm 0.0003$ mT and $\omega = (12 \pm 5) \times 10^{12}$ rad s^{-1}. Considering the large experimental errors involved, it practically overlaps the corresponding value obtained in the case of the B_2^0 parameters.

4.4. The temperature dependence of the hyperfine parameters

Although the relative variations are quite small, the absolute values of both $A_\parallel$ and $A_\perp$ hyperfine parameters exhibit a clear decrease with the temperature, as one can see in figures 5(a) and (b). Considering the hyperfine temperature variation to be influenced mostly by the presence

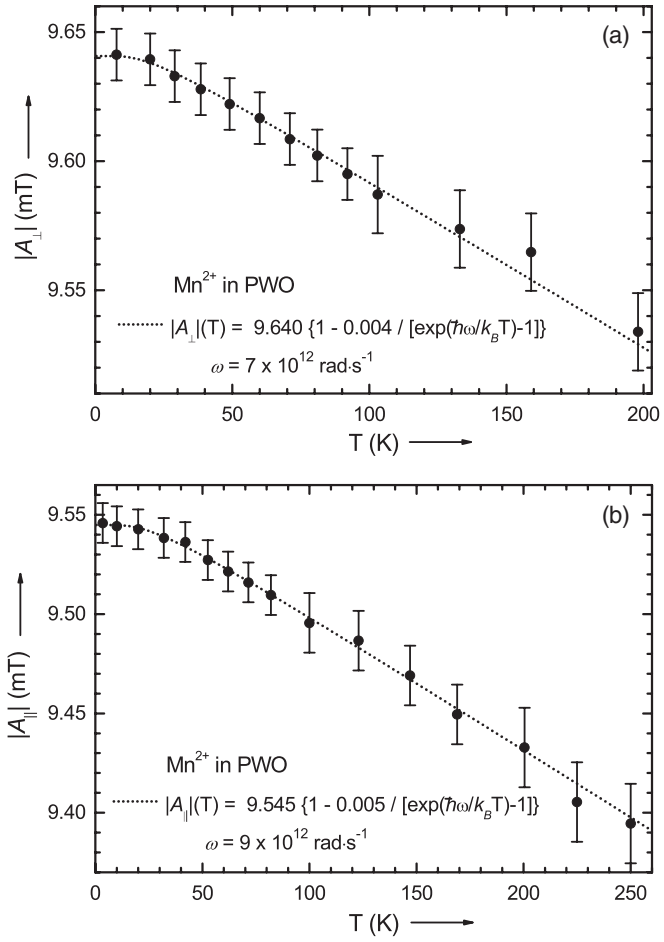

Figure 5. The temperature variation of the absolute value of the hyperfine (a) $A_\perp$ and (b) $A_\parallel$ parameters for the Mn^{2+} ions in PWO. Solid circles: experimental data. Dotted curve: simulated temperature dependence.

of a resonant mode, both $|A_\parallel|(T)$ and $|A_\perp|(T)$ could be well fitted with the formula

$$|A|(T) = \alpha_0 \left(1 - \frac{\alpha_1}{\exp(\hbar\omega/k_B T) - 1}\right). \tag{4}$$

Here α_0 is the hyperfine parameter value at 0 K and the second term in the brackets accounts for the coupling with a resonant mode of frequency ω. We obtained the best fit for $|A_\parallel|$ and $|A_\perp|$ with the frequency values $\omega = (9 \pm 2) \times 10^{12}$ and $(7 \pm 3) \times 10^{12}$ rad s^{-1}, respectively. The other fitting parameters were $\alpha_0 = 9.545 \pm 0.005$ mT and $\alpha_1 = 0.005 \pm 0.003$ for $|A_\parallel|$, and $\alpha_0 = 9.640 \pm 0.005$ mT and $\alpha_1 = 0.004 \pm 0.003$ for $|A_\perp|$. Moreover, the simulation of both $|A_\parallel|$ and $|A_\perp|$ using the same value $\omega = 8.8 \times 10^{12}$ rad s^{-1} determined from the $|B_2^0|$ temperature dependence proved to be still well within the experimental errors.

4.5. Linewidth temperature dependence. The spin–lattice relaxation

The EPR lines of the Mn^{2+} ions in PWO exhibit a clear broadening with increasing temperature. In order to gain information about the relaxation mechanism which seems very likely to be responsible for the line broadening, we determined the lineshape and linewidth temperature variation of one of the component lines belonging to the central sextet of the spectrum along the *c*-direction, thus avoiding the random stress broadening effects.

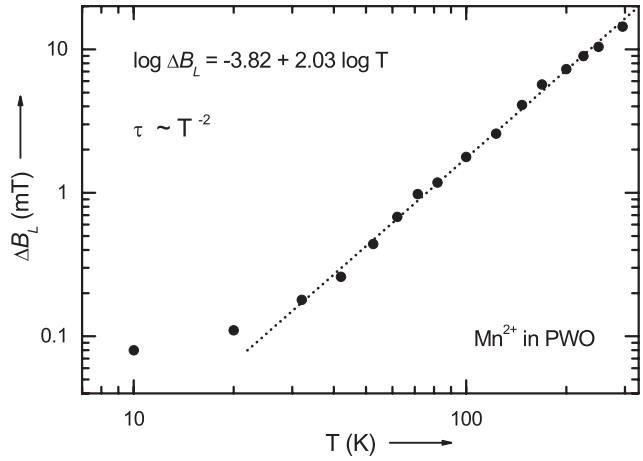

Figure 6. The temperature variation of the EPR linewidth for the Mn^{2+} ions in PWO (log–log scale). Solid circles: experimental data. Dotted line: simulated temperature dependence. The fitting has been performed only for temperatures where the lineshape is Lorentzian.

At low temperatures (up to 20 K) the lineshape was found to be pure Gaussian, which we attributed to inhomogeneous broadening effects. Above 20 K an increased Lorentzian contribution to the lineshape was observed. Above 60 K the lineshape was found to be purely Lorentzian, the lifetime broadening effect thus overcoming the other contributions to the lineshape.

The relaxation contribution to the linewidth associated with the lifetime broadening can be determined as [24]

$$\Delta B_{\mathrm{L}} = \Delta B_{\mathrm{pp}} - \Delta B_0 \tag{5}$$

where $\Delta B_0 = 0.062$ mT is the temperature independent inhomogeneous linewidth, measured as the peak-to-peak derivative linewidth at 3.4 K, where the line is purely Gaussian, and ΔB_{pp} is the observed peak-to-peak derivative linewidth at temperature T. The temperature variation of ΔB_{L} is proportional to the temperature variation of the inverse of the relaxation time, $1/\tau$ [13].

As shown in figure 6, in a log-to-log plot of $\Delta B_{\mathrm{L}}(T)$, the functional dependence of the relaxation time versus temperature was found to be proportional to T^{-2} for temperatures above 60 K. Such behaviour is expected for a Raman relaxation process, in which a resonant mode is involved [25]. At lower temperatures the ΔB_{L} temperature dependence is deviating from a T^{-2} law, very likely due to the mixed Lorentzian–Gaussian character of the lineshape—which makes the use of formula (5) questionable, as well as to the increased role of other spin–lattice relaxation mechanisms.

5. Conclusions

The analysis of the temperature variation of the ZFS and hyperfine parameters in the EPR spectrum of the Mn^{2+} ions in PWO crystals, as well as the high temperature Raman-type relaxation determined from the temperature induced line broadening above 60 K, points to the presence of a single, resonant mode, which is very likely due to the large mass difference between the substitutional Mn^{2+} impurity ions and the substituted Pb^{2+} host ions. The local vibrational mode at the Mn^{2+} impurity ions with a frequency $\omega = 8.8 \times 10^{12}$ rad s^{-1}, as most accurately determined from the temperature dependence of the B_2^0 parameter, is dominating

the spin–lattice interaction of the paramagnetic ion. Our analysis also indicates that, in the case of all spin Hamiltonian parameters with the exception of the g components, the role played by the intrinsic thermal expansion in their temperature dependence seems to be practically negligible.

The present results strongly suggest that the occurrence of local vibrational modes and their dynamic interaction with the impurity ions found in the PWO crystal lattice should be also taken into consideration in understanding the radiative processes in this material, especially in the case of impurities with a large difference of mass compared to the ions of the host lattice.

Acknowledgments

This work was performed in the frame of the bilateral Flemish–Romanian scientific research project BIL00/72, with support from the Romanian Ministry of Education and Research, through programme CERES (project no 4-76/2004). Partial financial support by the Flemish Fund for Scientific Research (FWO) in the group project G.0409.02, as well as of the Czech Science Foundation project 202/01/0753, is also gratefully acknowledged.

References

[1] Nikl M 2000 *Phys. Status Solidi* a **178** 595
[2] Kobayashi M, Usuki Y, Ishii M, Yazawa T, Hara K, Tanaka M, Nikl M and Nitsch K 1997 *Nucl. Instrum. Methods Phys. Res.* A **399** 261
[3] Baccaro S, Boháček P, Borgia B, Cecilia A, Dafinei I, Diemoz M, Ishii M, Jarolimek O, Kobayashi M, Martini M, Montecchi M, Nikl M, Nitsch K, Usuki Y and Vedda A 1997 *Phys. Status Solidi* a **160** R5
[4] Nikl M, Bohacek P, Nitsch K, Mihokova E, Martini M, Vedda A, Crocci S, Pazzi G P, Fabeni P, Baccaro S, Borgia B, Dafinei I, Diemoz M, Organtini G, Auffray E, Lecoq P, Kobayashi M, Ishii M and Usuki Y 1997 *Appl. Phys. Lett.* **71** 3755
[5] Nikl M, Bohacek P, Mihokova E, Solovieva N, Vedda A, Martini M, Pazzi G P, Fabeni P and Kobayashi M 2002 *J. Appl. Phys.* **91** 2791
[6] Bohacek P, Nikl M, Solovieva N and Trunda B 2004 *Radiat. Meas.* **38** 363
[7] Nistor S V, Stefan M, Goovaerts E, Nikl M and Bohacek P 2004 *Radiat. Meas.* **38** 655
[8] Wyckoff R W G 1951 *Crystal Structure* vols 2, 8 (New York: Interscience)
[9] Stefan M, Nistor S V, Goovaerts E and Schoemaker D 2004 *Phys. Rev.* B **69** 104107
[10] *Computer Program EPRNMR* version 6.5 Department of Chemistry, University of Saskatchewan, Canada
[11] Meilman M L 1966 *Fiz. Tverd. Tela* **8** 3656
[12] Rosa J, Asatryan H R and Nikl M 1996 *Phys. Status Solidi* a **158** 573
[13] Abragam A and Bleaney B 1971 *Electron Paramagnetic Resonance of Transition Ions in Crystals* (Oxford: Clarendon)
[14] Hempstead C F and Bowers K D 1960 *Phys. Rev.* **118** 131
[15] Samoilovich M I, Novozhilov A I and Potkim L I 1967 *Zh. Exp. Khim.* **8** 536
[16] Lyons D H and Kedzie R W 1966 *Phys. Rev.* **145** 148
[17] Walsh W M Jr, Jeener J and Bloembergen N 1965 *Phys. Rev.* **139** A1338
[18] Zdansky K 1968 *Phys. Status Solidi* **28** 181
[19] Pfister G, Dreybrodt W and Assmus W 1969 *Phys. Status Solidi* **36** 351
[20] Serway R A 1971 *Phys. Rev.* B **3** 608
[21] Barberis G E and Calvo R 1974 *Solid State Commun.* **15** 173
[22] Ishii M, Harada K, Kobayashi M, Usuki Y and Yazawa T 1996 *Nucl. Instrum. Methods Phys. Res.* A **376** 203
[23] Bjork R L 1957 *Phys. Rev.* **105** 456
[24] Stapleton H J and Brower K L 1969 *Phys. Rev.* **178** 481
[25] Klemens P G 1962 *Phys. Rev.* **125** 1795